British Journal of Pharmacology (2002) 136, 459–471

www.nature.com/bjp

Cardiac electrophysiologic and antiarrhythmic actions of a pavine alkaloid derivative, *O*-methyl-neocaryachine, in rat heart

[1]Gwo-Jyh Chang, *,[2]Ming-Jai Su, [2]Li-Man Hung & [3]Shoei-Sheng Lee

[1]Graduate Institute of Clinical Medicine, College of Medicine, Chang Gung University, Tao-Yuan, Taiwan; [2]Department of Pharmacology, College of Medicine, National Taiwan University, No 1, Sec 1, Jen-Ai Road, Taipei, Taiwan and [3]School of Pharmacy, College of Medicine, National Taiwan University, No 1, Sec 1, Jen-Ai Road, Taipei, Taiwan

1 *O*-methyl-neocaryachine (OMNC) suppressed the ischaemia/reperfusion-induced ventricular arrhythmias in Langendorff-perfused rat hearts ($EC_{50}=4.3$ μM). Its electrophysiological effects on cardiac myocytes and the conduction system in isolated hearts as well as the electromechanical effects on the papillary muscles were examined.

2 In rat papillary muscles, OMNC prolonged the action potential duration (APD) and decreased the maximal rate of depolarization (V_{max}). As compared to quinidine, OMNC exerted less effects on both the V_{max} and APD but a positive inotropic effect.

3 In the voltage clamp study, OMNC decreased Na^+ current (I_{Na}) ($IC_{50}=0.9$ μM) with a negative-shift of the voltage-dependent inactivation and a slowed rate of recovery from inactivation. The voltage dependence of I_{Na} activation was, however, unaffected. With repetitive depolarizations, OMNC blocked I_{Na} frequency-dependently. OMNC blocked I_{Ca} with an IC_{50} of 6.6 μM and a maximum inhibition of 40.7%.

4 OMNC inhibited the transient outward K^+ current (I_{to}) ($IC_{50}=9.5$ μM) with an acceleration of its rate of inactivation and a slowed rate of recovery from inactivation. However, it produced little change in the steady-state inactivation curve. The steady-state outward K^+ current (I_{SS}) was inhibited with an IC_{50} of 8.7 μM. The inward rectifier K^+ current (I_{K1}) was also reduced by OMNC.

5 In the perfused heart model, OMNC (3 to 30 μM) prolonged the ventricular repolarization time, the spontaneous cycle length and the atrial and ventricular refractory period. The conduction through the AV node and His-Purkinje system, as well as the AV nodal refractory period and Wenckebach cycle length were also prolonged (30 μM).

6 In conclusion, OMNC blocks Na^+, I_{to} and I_{SS} channels and in similar concentrations partly blocks Ca^{2+} channels. These effects lead to a modification of the electromechanical function and may likely contribute to the termination of ventricular arrhythmias. These results provide an opportunity to develop an effective antiarrhythmic agent with modest positive inotropy as well as low proarrhythmic potential.

British Journal of Pharmacology (2002) **136,** 459–471

Keywords: *O*-methyl-neocaryachine; electrophysiology; cardiac arrhythmia; ionic currents; cardiac myocytes; cardiac arrhythmia; quinidine

Abbreviations: AERP, atrial effective refractory period; AH, atrio-His bundle conduction interval; APA, action potential amplitude; $APD_{50,\ 90}$, action potential duration measured at 50 and 90% repolarization; AVNERP, AV nodal effective refractory period; BCL, basic cycle length; G, conductance; HPFRP, His-Purkinje system functional refractory period; HV, His-ventricular conduction interval; I_{Ca}: Ca^{2+} inward current; I_{K1}: inward rectifier K^+ current; I_{Na}: Na^+ inward current; I_{SS}: steady-state outward K^+ current; I_{to}: transient outward K^+ current; k, slope factor; OMNC, *O*-methyl-neocaryachine; RMP, resting membrane potential; SA, sinoatrial conduction interval; τ, time constant; τ_f and τ_s, fast and slow time constant; VERP, ventricular effective refractory period; V_h, half-maximal potential; V_{max}, maximal upstroke velocity of action potential; VRT, ventricular repolarization time; WCL, Wenckebach cycle length

Introduction

Ischaemic heart disease remains a serious problem despite intensive research in recent years. Patients with ischaemic heart disease are particularly susceptible to events of ventricular tachycardia that may even culminate in sudden cardiac death. Class I antiarrhythmic drugs have been used for the treatment of life-threatening ventricular tachyarrhythmias. However, the effectiveness of most currently used drugs has always been limited by serious cardiac depression or proarrhythmic effects (Woosley, 1991). The CAST (1989) study provided evidence that some class I_C agents (such as flecainide and encainide) significantly increased postinfarction mortality. Thus, the role of class I drugs in controlling serious arrhythmias is diminishing. In the search for new drugs with a more favourable benefit-risk ratio, substances that prolong the cardiac APD and, as a result, the effective refractory period (ERP) (class III like drugs) have received considerable attention as potential antiarrhythmic agents

*Author for correspondence; E-mail: mjsu@ha.mc.ntu.edu.tw

(Woosley, 1991; Hondeghem, 1992). The antiarrhythmic benefit afforded by class III like agents is proposed to result from sufficient prolongation of myocardial refractoriness for the wave length activation to exceed the path length of the re-entrant circuit, thereby preventing the initiation or maintenance of re-entrant excitation (Wellens *et al*., 1984). Clinical results with *d*-sotalol, a 'pure' class III agent, however, highlighted the limited utility of this type of agent, because it causes torsade de pointes arrhythmias, and even may increase mortality in subsets of patients with myocardial infarction and lowered ejection fraction (Waldo *et al*., 1996). Accordingly, the search for new types of antiarrhythmic drugs to treat such life-threatening arrhythmias remains an important area of investigation. More recently, there has also been much attention given to compounds possessing a multiple mode of action, with the expectation that such agents may be devoid of serious untoward cardiac side effects (Mátyus *et al*., 1997).

The pavine alkaloids are derived biogenically from benzylisoquinolines (Gözler *et al*., 1983) and usually exist in plants of Lauraceae (Tomita *et al*., 1966). Pavines have been shown to possess many biological activities such as behavioural effects (Meisenberg *et al*., 1984) and antitumour effects (Wu *et al*., 1989). Recently, by using large-scale screening tests, we found that *O*-methyl-neocaryachine (OMNC, Figure 1A), a pavine alkaloid derivative, has been shown to convert the ischaemia/reperfusion induced arrhythmias in rat hearts. We have therefore evaluated its electrophysiological and mechanical actions. Our results define its effects on the conduction system of isolated Langendorff-perfused rat hearts, as well as its effects on the ionic currents of cardiac myocytes.

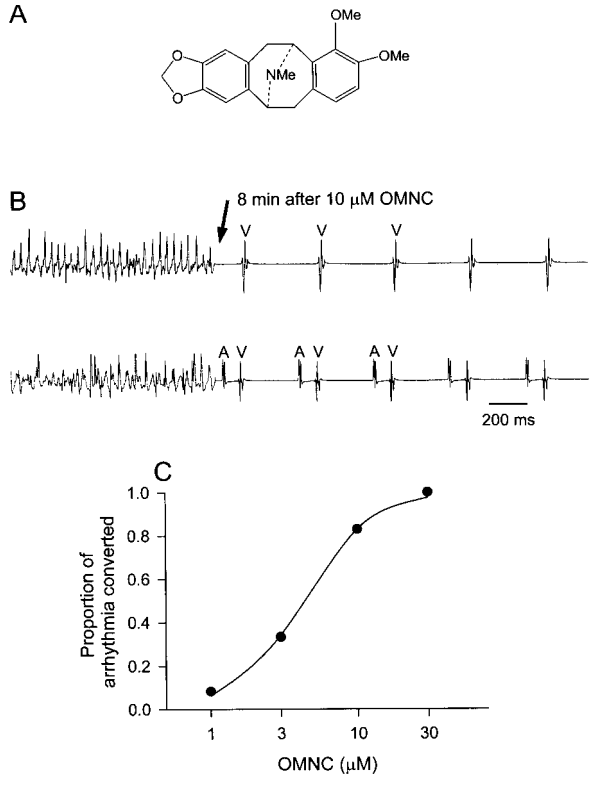

Figure 1 (A) Chemical structure of *O*-methyl-neocaryachine (OMNC). (B) Conversion of polymorphic ventricular tachyarrhythmia induced by ischaemia-reperfusion to normal sinus rhythm by OMNC. Upper panel shows the ventricular electrogram. The electrogram of the lower panel was recorded at lower right atrium and shows the atrial (A) and ventricular depolarization (V). (C) Antiarrhythmic efficacy of OMNC at various concentrations is plotted against the drug concentration. Antiarrhythmic efficacy is expressed as the proportion of conversion of the ventricular tachyarrhythmia to normal sinus rhythm.

Methods

Induction and conversion of ischaemia-reperfusion-induced arrhythmias

All experimental protocol were approved by the animal use committee of our institution. Adult male Wistar-Kyoto (WKY) rats weighing 200–300 g (purchased from the Laboratory Animal Center, Taiwan University Medical College) were anaesthetized with sodium pentobarbitone (50 mg kg^{-1}, i.p.) and given heparin (300 units kg^{-1}, i.p.) and then sacrificed by cervical dislocation. The Langendorff-perfused heart model with constant pressure instead of constant flow was used (Curtis & Hearse, 1989). The rat hearts were excised immediately and mounted on a Langendorff apparatus and perfused *via* the aorta with normal Tyrode solution. The solution was continuously gassed with 95% O_2 and 5% CO_2 to give a pH of 7.4 and was maintained at 37°C. The electrograms were recorded from a low atrial and a ventricular recording electrode. The signals were continuously monitored on an oscilloscope (54503A, Hewlett-Packard Co., Boise, Ida., U.S.A.) and pertinent data recorded on a two-channel chart recorder (RS 3200, Gould Inc., Cleveland, Ohio, U.S.A.). The left anterior descending coronary artery was ligated for 20 min before the release of the ligature. The establishment of ischaemia and reperfusion was ascertained by the amount of coronary effluent. A successful occlusion was confirmed by 40–50% reduction in coronary flow as compared with pre-ischaemic values. The antiarrhythmic effect of the compound was tested after arrhythmias had been induced and persisted for at least 5 min.

Electromechanical measurements on papillary muscles

The papillary muscles from the left ventricles of the rat hearts about 0.5–1 mm in diameter and 3–5 mm in length were dissected and mounted in a tissue chamber (STEIRT, HSE (Hugo Sachs Electronik), March-Hugstetten, Germany) of 2 ml volume and superfused at a rate of 25 ml min^{-1} with normal Tyrode solution. The solution was continuously gassed with 95% O_2 and 5% CO_2 to give a pH of 7.4 and was maintained at 37°C. One end of the papillary muscle was hooked to a force-displacement transducer (Type F30, HSE), and the other end was fixed to the bottom of the tissue chamber. The preparations were stimulated at a rate of 1 Hz through the platinum field electrodes. Stimuli were rectangular pulses of 2 ms duration at twice the threshold voltage, delivered from an electronic stimulator (PULSEMASTER A300, WPI, Sarasota, FL, U.S.A.). Each preparation was stretched to a length at which maximum developed force was evoked and allowed to equilibrate for at least 1 h before the commencement of the experiments. Transmembrane potentials were recorded using conventional microelectrode techniques.

Microelectrodes filled with 3 M KCl having tip resistances 15–25 MΩ were connected to the input of a high impedance, capacity neutralizing amplifier (Axoclamp 2B, Axon Instruments Inc., Foster City, CA, U.S.A.). Records were digitized using an A/D converter (Digidata 1200, Axon) and continuously displayed and stored on an online computer. The mechanical response was also simultaneously recorded on a Gould chart recorder. Action potential and contractile force were analysed by pCLAMP software (Version 6.0, Axon).

Whole cell patch clamp recording

Single ventricular myocytes were isolated from heart of adult WKY rats by enzymatic dissociation according to a procedure previously described (Mitra & Morad, 1985; Chang *et al*., 1996). Ionic currents were studied in whole-cell configuration at room temperature (25–27°C) (Hamill *et al*., 1981). Only quiescent rod-shaped cells lacking membrane deformities and showing clear cross striations were studied. A small aliquot of the solution containing the isolated cells was placed in a 1 ml chamber mounted on the stage of a Nikon Diaphot inverted microscope (Nikon, Tokyo, Japan). Borosilicate glass electrodes (O.D.: 1.5 mm) were used, with tip resistance of 2–5 MΩ when filled with the appropriate internal solution. Membrane currents were recorded with a Dagan 8900 patch/whole cell clamp amplifier (Dagan Corp., Minneapolis, MN, U.S.A.). Command pulses were generated by a 12-bit Digidata 1200 D/A converter controlled by pCLAMP software. Data were low pass filtered at 10 kHz with a four-pole Bessel filter (FL4, Dagan) and digitized at 20 kHz, and then stored on the hard disk of an IBM-compatible computer. After forming the whole-cell recording configuration, a capacitive transient induced by a 10 mV step from a holding voltage of 0 mV was recorded and used for the calculation of cell capacitance. Cell capacitances were estimated from integration of capacitative current transients and had the mean values of 132.5 ± 14.1 pF ($n = 24$). Series resistance (R_s) was in the range of 4–6 MΩ and was compensated by 60 to 80%. For measurement of Ca^{2+} and Na^+ inward currents, the K^+ currents were blocked by adding CsCl (2–4 mM) to the bathing medium and internal dialysis of the cells with Cs^+ and TEA-containing pipette solution. Experiments on steady-state I_{Na} inactivation were studied in a Co^{2+}-containing (1 mM) low Na^+ Tyrode solution ($[Na^+] = 54$ mM, with NaCl replaced by N-methyl-D-glucamine) and dialysis of the cell with Na^+ containing (10 mM) Cs^+ pipette solution. In experiments to measure K^+ currents, contamination by I_{Na} and I_{Ca} was prevented by addition of TTX (30 μM) and Co^{2+} (1 mM), respectively. Data were enrolled from those experiments performed in cells where the estimated voltage error attributed to uncompensated R_s ($R_s \times I_{Na}$) was below 5 mV. Data acquisition and analysis were performed using the Clampex and Clampfit module of pCLAMP software, respectively Sigmaplot 4.0 (Jandel Scientific) was used for fitting data with Boltzmann or other user-defined functions.

Intracardiac electrocardiogram recording experiment

Animal preparation The rat heart including part of the superior and inferior vena cava and the ascending aorta was quickly excised *via* thoracotomy. The aorta was retrogradely perfused at a rate of 4 ml $min^{-1}g^{-1}$ cardiac tissue with normal Tyrode solution. The solution was continuously gassed with 95% O_2 and 5% CO_2 to give a pH of 7.4 and was maintained at 37°C. The endocardial surface of the right atrium was exposed *via* a small incision along the anterolateral atrioventricular groove. For His bundle electrogram (HBE) recording, a silver electrode connected to a tungsten spring was placed on the endocardium near the apex of the triangle of Koch to record the HBE. In order to obtain a recognizable T wave and a ventricular depolarization wave simultaneously on the ventricular electrogram, the tips of the ventricular recording electrode were separated and placed on opposite sides of the ventricular epicardium near the ventricular apex. High right atrial pacing electrode was placed near the junction of the superior vena cava and right atrium. The ventricular pacing electrode was placed on the pericardium near the right ventricular apex. Pacing studies were performed by utilizing a programmable stimulator (DTU 215, Bloom Associated Ltd, PA, U.S.A.). A pacing stimulus of 1 ms in duration and twice the threshold voltage was applied to the preparation through the bipolar atrial or ventricular electrodes. The signals were continuously monitored on an oscilloscope (54503A, Hewlett Packard, U.S.A.) and pertinent data recorded on a two-channel Gould chart recorder with a paper speed of 100 mm s^{-1}.

Experimental protocol Electrophysiological studies were performed according to standard methods described previously (Josephson & Seides, 1979). The average of four stable cycle lengths of spontaneous heart beats was taken as the pacemaker automaticity, which could be a sinus or an atrial pacemaker. The right atrium was then paced at a constant rate which was slightly faster than the spontaneous heart rate. At this constant rate pacing, the intra-atrial conduction time (SA), AV nodal conduction time (AH), His-Purkinje conduction time (HV) and ventricular repolarization time (VRT) were measured.

Incremental right atrial pacing was used to determine the Wenckebach cycle length. The atrial pacing cycle length was decreased (every 5–10 s) in steps of 10–20 ms until a stable 1:1 AV nodal conduction pattern was lost. The longest pacing cycle length at which a 1:1 AV conduction could not be maintained (either 2:1 conduction or Wenckebach cycle) was defined as the Wenckebach cycle length.

An atrial premature extra-stimulation (S_2) was then delivered to the high right atrium after a train of constant rate atrial pacing (S_1S_1) for eight beats. This atrial extra-stimulation (S_1S_2) interval was decreased in 10 ms-step until the atrial refractory period was reached. The following data were obtained: Atrial effective refractory period (AERP) was the longest S_1S_2 interval that did not evoke an atrial depolarization wave A_2. AV nodal effective refractory period (AVNERP) was the longest S_1S_2 interval in which the evoked A_2 failed to evoke a His bundle depolarization wave H_2. The longest H_1H_2 interval that failed to evoke a premature ventricular depolarization was defined as the His-Purkinje effective refractory period (HPERP).

The ventricular extrastimulation study protocol was similar to the atrial extrastimulation study. The ventricular effective refractory period (VERP) was defined as the longest S_1S_2 interval that failed to evoke a premature ventricular depolarization.

Solutions and drugs

The normal Tyrode solution contained (in mM): NaCl 137.0, KCl 5.4, $MgCl_2$ 1.1, $NaHCO_3$ 11.9, NaH_2PO_4 0.33, $CaCl_2$ 1.8 and dextrose 11.0. The HEPES-buffered Tyrode solution contained (in mM): NaCl 137.0, KCl 5.4, KH_2PO_4 1.2, $MgSO_4$ 1.22, $CaCl_2$ 1.8, dextrose 11.0, and HEPES 6.0, titrated to pH 7.4 with NaOH. The internal pipette filling solution contained (in mM): KCl 120.0, NaCl 10.0, MgATP 5.0, EGTA 5.0, and HEPES 10.0, adjusted to pH 7.2 with KOH. The Cs^+-containing pipette solution contained (in mM): CsCl 130.0, EGTA 5.0, tetraethylammonium (TEA) chloride 15.0, dextrose 5.0 and HEPES 10.0, adjusted to pH 7.2 with CsOH. OMNC hydrochloride was synthesized by one of the authors, Dr S. S. Lee. Its purity (>99%) was confirmed by spectral methods (mass and NMR). Quinidine sulphate and tetrodotoxin (TTX) were purchased from Sigma Chem. Co. Stock solutions (50 mM) of OMNC hydrochloride and quinidine sulphate were prepared in distilled water and further dissolved in perfusion medium immediately before experimentation. Drugs were administered in a cumulative manner.

Data analysis and statistics

Values are expressed as the means ± s.e.mean. A repeated-measures analysis of variance followed by the Tukey test was used to examine the significance of changes after the drug. Since the drug was added in cumulative manner, only the significance ($P<0.05$) between the control and the experimental values at each concentration was indicated by asterisks. Concentration-response curves were fitted by an equation of the form:

$$E = E_{max}/[1 + (IC_{50}/C)^{n_H}] \quad (1)$$

where E is the effect at concentration C, E_{max} is maximal effect, IC_{50} is the concentration for half-maximal block and n_H is the Hill coefficient. The inactivation curves of I_{Na} or I_{to} were fitted by the Boltzmann equation:

$$I/I_{max} = 1/\{1 + \exp[(V_m - V_h)/k]\} \quad (2)$$

where I gives the current amplitude and I_{max} its maximum, V_m the potential of prepulse, V_h the half-maximal inactivation potential, and k the slope factor.

Results

Antiarrhythmic efficacy on reperfusion arrhythmias

At a concentration of 1 to 30 μM, OMNC was able to convert a polymorphic ventricular tachyarrhythmia induced by ischaemia-reperfusion experiment model (Figure 1B, C). In the control heart preparations, following 20-min occlusion of left coronary artery, reperfusion elicits arrhythmias within 5–10 s which was maintained for about 85.6 ± 14.5 min ($n=14$ hearts). Figure 1B shows a typical trace for the conversion of ventricular tachyarrhythmia induced by reperfusion after a 20-min occlusion period to normal sinus rhythm by 10 μM OMNC. Drugs were administered in a cumulative manner, and it took about 5–8 min for a given effective concentration to terminate the arrhythmias. Out of 12 hearts ($n=12$) with sustained ventricular tachyarrhythmia induced by ischaemia-reperfusion, OMNC 1 μM converted one heart to normal sinus rhythm, 3 μM converted three of the remaining 11 hearts and 10 μM converted six of the other eight hearts and 30 μM converted two of the other two hearts to normal sinus rhythm. The concentration-response curve for arrhythmia conversion showed an EC_{50} of 4.3 μM (Figure 1C). During perfusion with a given effective concentration of OMNC for about 1.5–2 h, no new tachyarrhythmias were observed in these experiments. Quinidine caused a comparable degree of antiarrhythmic potency. Out of nine hearts ($n=9$) with sustained ventricular tachyarrhythmias, quinidine 3 μM converted the tachyarrhythmia to normal sinus rhythm in three hearts, 10 μM converted five of the remaining six hearts and 30 μM converted the remaining one heart to normal sinus rhythm. The calculated EC_{50} for arrhythmia conversion was 4.1 μM.

Electromechanical effects of OMNC on papillary muscles

The representative changes in action potential and contractile force before and after OMNC in a rat ventricular papillary muscle driven at 1 Hz are shown in Figure 2. The mean data are summarized in Table 1. It can be observed that OMNC prolonged the action potential duration at 50 and 90% repolarization (APD_{50} and APD_{90}) and decreased the maximal upstroke velocity of depolarization (V_{max}) in a concentration-dependent manner. At the same time, the contractile force was increased. The action potential amplitude and resting membrane potential were not significantly affected by OMNC. The effect of OMNC was reversed after 10–15 min of washout with control solution. As compared with quinidine, OMNC caused less pronounced effects on the APD and V_{max} (Figure 2 and Table 1). However, quinidine depressed the contractility at higher concentrations (e.g., 100 μM).

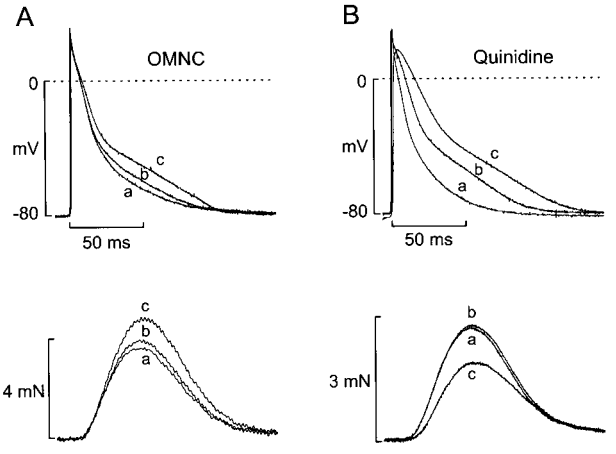

Figure 2 Original records of transmembrane action potential and isometric contraction in rat papillary muscles driven at 1 Hz before and during application of cumulatively increasing concentrations of OMNC (A) and quinidine (B). Each concentration was allowed to act for 15–20 min before the record was taken. a, b, and c indicate control, and during superfusion with 30 and 100 μM drugs, respectively.

Table 1 Effects of *O*-methyl-neocaryachine (OMNC) (A) and quinidine (B) on the action potential parameters and contractile force in rat ventricular papillary muscles driven at 1 Hz

		RMP (mV)	*APA* (mV)	V_{max} (V/s)	APD_{50} (ms)	APD_{90} (ms)	*CF* (mN)
A ($n=8$)							
Control		−80.6±0.9	106.2±1.9	234.4±12.3	15.8±1.7	57.3±4.6	3.3±0.2
OMNC	3 μM	−80.5±1.0	105.4±1.7	231.5±11.7	15.9±1.8	57.6±4.7	3.4±0.2
	10 μM	−80.2±1.2	104.9±1.9	220.8±13.5	16.3±1.8	62.3±5.5	3.5±0.2
	30 μM	−79.3±1.3	104.5±2.2	206.5±13.8	18.1±1.9	70.3±5.5	3.6±0.2
	100 μM	−77.1±1.6	99.7±2.3*	174.2±17.2**	23.6±2.6*	83.2±6.1**	4.0±0.2*
Wash		−80.2±1.7	103.7±1.6	232.4±13.2	16.3±1.5	62.1±4.7	3.2±0.2
B ($n=6$)							
Control		−82.3±1.1	111.9±2.1	283.8±24.0	11.3±1.1	47.9±6.1	3.1±0.3
Quinidine	3 μM	−80.8±1.6	109.1±2.9	258.0±15.3	12.3±1.4	51.4±7.1	3.1±0.3
	10 μM	−80.8±1.3	107.4±2.7	252.3±20.4	14.1±1.0	56.8±6.9	3.1±0.3
	30 μM	−80.1±1.5	104.6±2.9	211.7±20.8*	21.2±1.4#	73.5±6.8*	3.2±0.3
	100 μM	−80.5±1.6	101.1±1.8#	137.2±7.1#	34.2±1.8#	96.8±6.2#	2.5±0.2
Wash		−80.6±1.6	106.5±1.6	187.3±23.0**	15.4±1.7#	74.7±3.9**	3.3±0.2

Values are means±s.e.mean RMP, resting membrane potential; APA, action potential amplitude; V_{max}, maximal upstroke velocity of phase 0 depolarization; APD_{50} and APD_{90}, action potential duration measured at 50 and 90% repolarization, respectively; CF, contractile force. $^*P<0.05$, $^{**}P<0.01$ and $\#P<0.001$ as compared with the respective control.

Effects of OMNC on L-type calcium current (I_{Ca})

To activate I_{Ca}, 120 ms pulses to 0 mV from a holding potential of −40 mV (to inactivate I_{Na} and T-type Ca^{2+} current) were delivered at 0.2 Hz. A time-dependent reduction of I_{Ca} ('rundown' phenomenon) was observed during the initial 10–15 min access of the patch pipette to the interior of the ventricular myocytes. Therefore, recordings were performed only on those cells with steady-state Ca^{2+} currents 15 min after cell rupture. A dose-dependent decrease in the Ca^{2+} currents was observed after OMNC (Figure 3Aa). The effect on I_{Ca} was reversible after 5–8 min washout of drug. The application of 3 and 10 μM OMNC reduced the I_{Ca} amplitude from 1.46 to 1.29 and 0.96 nA, respectively. The concentration-response curve of the effect of OMNC on the peak I_{Ca} is shown in Figure 3Ab. The data points were fitted according to the Hill equation. The mean IC_{50} calculated from the dose-response curve was 6.6±1.5 μM ($n=6$) with a maximal inhibition E_{max} of 40.7±4.9% ($n_H=1.28\pm0.33$). Peak I_{Ca} decreased by 17±4, 40±3, 73±2 and 86±3% ($n=6$) after 1, 3, 10 and 20 μM quinidine. The calculated IC_{50} for quinidine was 4.5±0.6 μM (maximal inhibition = 102±6%, $n_H=1.20\pm0.16$).

Effects of OMNC on sodium inward current (I_{Na})

After blocking the K^+ current with internal and external Cs^+ and blocking the Ca^{2+} current with external Co^{2+}, large fast inward currents were elicited by depolarization of the membrane (15 ms long) from a holding potential of −80 mV to −20 mV at 0.2 Hz. Figure 3Ba shows superimposed traces of I_{Na} obtained from a rat ventricular cell in the absence and presence of OMNC. OMNC blocked I_{Na} concentration-dependently (Figure 3Bb). The mean IC_{50} was 0.9±0.1 μM ($n=9$), with an average E_{max} of 99.9±0.9% inhibition and a mean n_H of 1.06±0.93. Peak I_{Na} also decreased by 21±3, 46±4, 79±4 and 94±1% ($n=8$) after 0.3, 1, 3, 10 μM quinidine. The estimated IC_{50} for quinidine was 1.3±0.2 μM (maximal inhibition = 104±1%, $n_H=1.16\pm0.07$). OMNC did not significantly modify the inactivation rate of I_{Na}. The decay of I_{Na} at −20 mV was well fitted to the biexponential functions (Figure not shown). The I_{Na} decay under control conditions ($n=9$) showed two time constants of $\tau_f=1.25\pm0.08$ ms and $\tau_s=6.47\pm0.95$ ms. Comparative values in the presence of 1 μM OMNC were $\tau_f=1.47\pm0.20$ ms and $\tau_s=6.13\pm0.62$ ms ($P>0.05$ for τ_f and τ_s) and 3 μM OMNC were $\tau_f=1.52\pm0.22$ ms and $\tau_s=6.68\pm1.34$ ms ($P>0.05$ for τ_f and τ_s), respectively.

To clarify the possible mechanisms of OMNC-induced reduction of I_{Na}, we studied the current-voltage relation for this current. From a holding potential of −80 mV, I_{Na} was elicited by depolarizing pulses to potentials ranging from −70 to +40 mV. The traces in Figure 4A show superimposed records of the currents obtained before and after superfusion with 0.3 and 1 μM OMNC. The current-voltage (I-V) relationships for I_{Na} under the three conditions are illustrated in Figure 4B. Under control condition, I_{Na} was activated at the threshold potential of around −60 mV and attained its maximum around −30 mV. OMNC blocked the Na^+ channel without causing significant changes in the I-V relationship. Conductance of Na^+ channel (G_{Na}) was then calculated according to

$$G_{Na} = I_{Na}/(E_m - E_{rev}) \quad (3)$$

where I_{Na} is the peak Na^+ current, E_{rev} is the reversal potential of this current, and E_m is the membrane potential. In Figure 4C, the normalized peak conductance of the Na^+ channel was plotted as a function of E_m. Data were analysed by using the Boltzmann equation as follows:

$$G_{Na}/G_{Na,\,max} = 1/\{1+\exp[(V_h - V_m)/k]\} \quad (4)$$

where V_h and k represent the voltage of activation midpoint and a slope factor, respectively. OMNC did not affect the voltage dependence for activation (Figure 4C). On average ($n=5$), $V_h=-45.9\pm1.1$ mV and $k=3.8\pm0.2$ mV under control conditions, and $V_h=-44.9\pm1.0$ mV and $k=4.4\pm0.2$ mV ($P>0.05$ for V_h and k) in the presence of

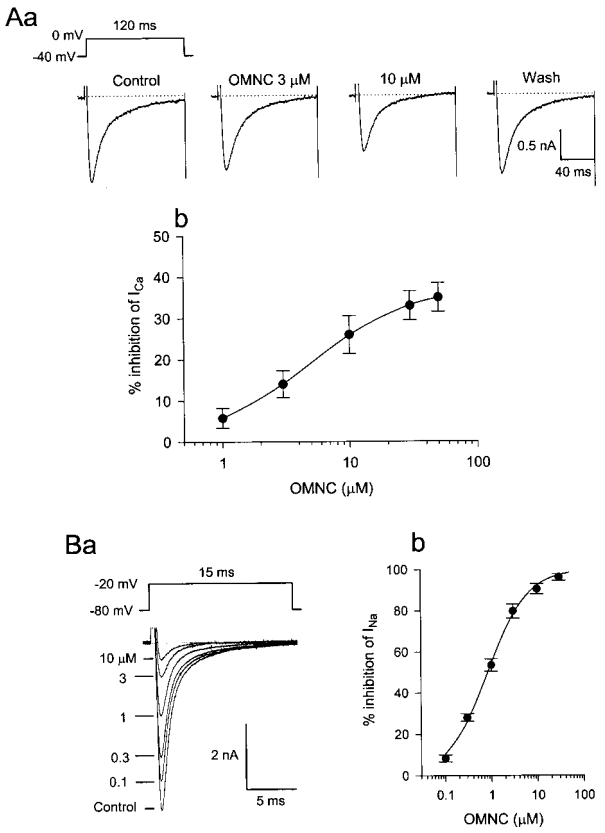

Figure 3 (A) Effect of OMNC on I_{Ca}. (Aa) The original records of I_{Ca} elicited by 120 ms step depolarizations (applied every 5 s) from a holding potential of -40 to 0 mV under control conditions, after 5-min cumulative superfusion with 3 and 10 μM OMNC and washout conditions. The horizontal dashed line indicates zero current level. (Ab) Concentration-response curve for the effect of OMNC on I_{Ca}. Percentage inhibition of peak corresponding to the control value was plotted against drug concentration. Symbols represent means$\pm$s.e.mean ($n=6$). The solid line was drawn by fitting to the Hill equation. (B) Concentration-dependent effect of OMNC on I_{Na}. (Ba) The original superimposed records of I_{Na} elicited by 15 ms step depolarizations from a holding potential of -80 mV to -20 mV under control conditions and after superfusion with OMNC. (Bb) Concentration-response curve for the inhibition of OMNC on I_{Na}. Each data point indicates means$\pm$s.e.mean ($n=9$).

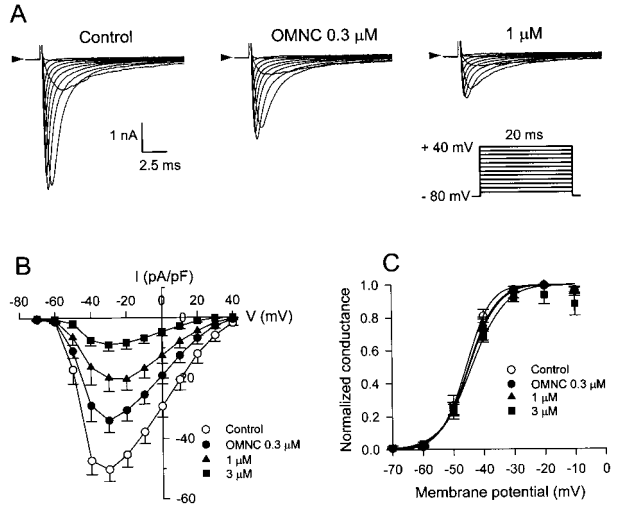

Figure 4 Effect of OMNC on I_{Na}. (A) The original superimposed records of I_{Na} elicited by 20 ms step depolarizations (applied at 10 mV increments every 5 s) from a holding potential of -80 mV to various potential levels ranging from -70 to $+40$ mV under control conditions, after 5-min superfusion with 0.3 and 1 μM OMNC. Arrow head in each panel indicates zero current level. (B) The *I-V* relationship for I_{Na} observed in the absence and during exposure of OMNC. Each data point represents means$\pm$s.e.mean from five cells. (C) Normalized Na^+ conductance ($G_{Na}/G_{Na,\ max}$) is plotted as a function of the membrane potential. The solid curves are drawn according to the Boltzmann equation (see text). Each data point indicates means$\pm$s.e.mean ($n=5$).

1 μM OMNC and $V_h=-43.8\pm1.0$ mV and $k=4.5\pm0.3$ mV in the presence of 3 μM OMNC ($P>0.05$ for V_h and k).

Effects of OMNC on voltage dependent steady-state inactivation and recovery from inactivation of Na^+ channel

To study the effect of OMNC on the voltage-dependent I_{Na} availablity, a double pulse experiment was carried out by applying a 20 ms test pulse to -20 mV following a 1000 ms conditioning prepulse to various potential levels ranging from -150 to -50 mV in 10 mV steps (Figure 5). Test I_{Na} traces were superimposed during both control and 3 μM OMNC superfusions (Figure 5A). The amplitude of I_{Na} elicited at conditioning potential of -130 mV decreased by 12.4 ± 5.6, 33.6 ± 5.6 and 63.0 ± 4.6% ($n=5$) after 1, 3 and 10 μM OMNC. The steady-state Na^+ channel inactivation curves were obtained by normalizing I_{Na} amplitudes to their maximum value and plotted as a function of prepulse membrane potential (Figure 5B). OMNC appeared to block the Na^+ current by causing a negative shift of the steady-state inactivation without affecting the slope factor. On average ($n=5$), $V_h=-91.4\pm3.9$ mV and $k=-6.0\pm0.5$ mV under control conditions, and $V_h=-98.5\pm3.8$ mV and $k=-6.3\pm0.7$ mV ($P>0.05$ for V_h and k) in the presence of 1 μM OMNC, $V_h=-104.4\pm4.0$ mV ($P<0.05$) and $k=-6.6\pm0.6$ mV ($P>0.05$) in the presence of 3 μM OMNC and $V_h=-114.4\pm2.4$ mV ($P<0.001$) and $k=-6.6\pm0.6$ mV ($P>0.05$) in the presence of 10 μM OMNC.

The effect of OMNC on the speed of I_{Na} recovery from inactivation was assessed using the protocol shown in the inset of Figure 6A. A 20 ms prepulse (I_p) was followed by a variable recovery period and a 20 ms test pulse (I_t) to assess the amount of current recovered. Each two pulse sequence was separated by a 30 s interval. Original current traces in the absence and presence of OMNC (1 μM) are shown in the lower panel of Figure 6A. The peak current for each test pulse was normalized to that for the prepulse and plotted as a function of recovery time (Figure 6B). Under control conditions, the I_{Na} recovered rapidly, being well described by the sum of two exponentials. In the presence of OMNC, the time courses of recovery (both τ_f and τ_s) were prolonged markedly. The proportion of the fast component of the recovering current was not affected by this agent. On average ($n=8$), $\tau_f=41.2\pm6.0$ ms and $\tau_s=182.9\pm24.8$ ms under control conditions, and $\tau_f=69.1\pm10.9$ ms ($P<0.05$) and $\tau_s=419.6\pm75.9$ ms ($P<0.01$) in the presence of 1 μM OMNC and $\tau_f=81.4\pm13.3$ ms ($P<0.01$) and $\tau_s=443.4\pm72.9$ ms ($P<0.01$) in the presence of 3 μM OMNC.

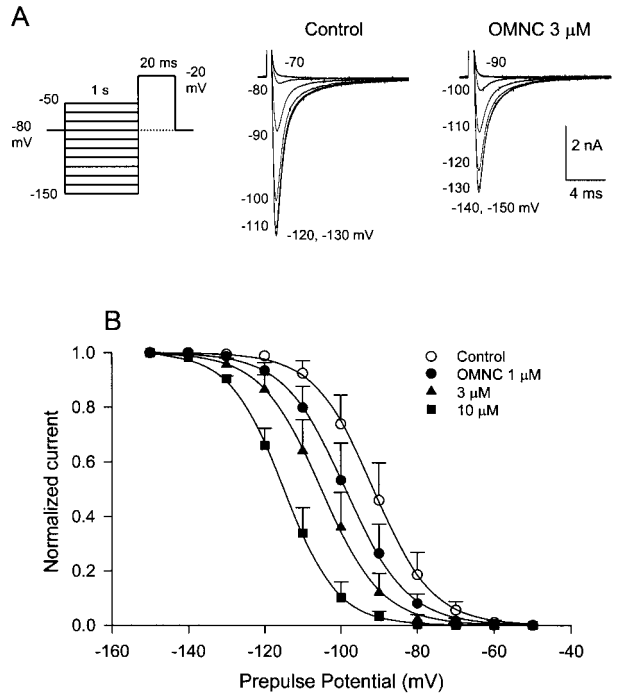

Figure 5 (A) Effects of OMNC on voltage-dependent steady-state inactivation of I_{Na}. (A) The clamp protocol is illustrated in the inset. A 1000 ms conditioning pulse was applied from the holding potential of −80 mV to various potentials ranging from −150 to −50 mV, which was followed by a test pulse to −20 mV. Test current traces under control conditions (left) and after 5-min superfusion with 3 μM OMNC (right) are shown. (B) The steady-state inactivation curves for I_{Na} were obtained by normalizing the current amplitudes (I) to the maximal value (I_{max}) and plotted as a function of the conditioning potentials in each condition ($n=5$). The line drawn through the data points was the best fit to the Boltzmann equation.

Tonic and use-dependent effects of OMNC on I_{Na}

To study the use-dependent block, cardiac myocytes were stimulated by trains of repetitive stimuli at varying rates. Figure 7A shows the superimposed records of I_{Na} obtained on the repetitive depolarizing pulses at a rate of 1 and 4 Hz. The amplitude of I_{Na} induced by each pulse successively applied is plotted in Figure 7B. In the absence of the drug, 16 successive pulses to −20 mV for 15 ms produced no significant decrease in I_{Na}, even at a high frequency of 4 Hz. In the presence of OMNC (1 μM), the amplitude of I_{Na} evoked by the first pulse in the pulse train was reduced from control value of 4.33±0.15 nA to 2.26±0.24 nA ($n=6$, $P<0.01$) at 1 Hz and from 4.22±0.19 nA to 2.12±0.30 nA ($n=6$, $P<0.01$) at 4 Hz, respectively. On the subsequent pulses, the I_{Na} amplitude became smaller and smaller and then reached the steady-state level. High frequency stimulation enhanced this extra-block. The averaged current amplitudes elicited by the first pulse and the steady-state were 2.26±0.24 nA and 2.07±0.24 nA ($n=6$, $P>0.05$) at 1 Hz and 2.12±0.30 nA and 1.22±0.25 nA ($n=6$, $P<0.05$) at 4 Hz, respectively.

Effects of OMNC on K^+ currents

In order to separate the K^+ outward current from overlapping currents, Na^+ and Ca^{2+} current was blocked with 30 μM TTX and 1 mM Co^{2+}, respectively. Typical current traces recorded in response to depolarizing and hyperpolarizing clamp steps to test potentials between +60 and −140 mV from a holding potential of −80 mV are shown in Figure 8A. Addition of OMNC (10 μM) to the superfusion solution reduced the amplitude of peak outward K^+ current (I_{to}) and accelerated its inactivation time course. In addition, OMNC also reduced the steady-state K^+ outward current (I_{SS}) at the end of 400 ms long clamp steps. Inward K^+ currents through the inward rectifier K^+ channel (I_{K1}) were also inhibited, although to a lesser degree. This effect was reversible after washout of the drug. Figure 8B, C show the current-voltage relation for the I_{to} and I_{SS} before, during and after washout of 10 μM OMNC, respectively. Figure 8D shows that the per cent inhibition of I_{to} integral by 10 μM OMNC was not significantly dependent on step potential.

The effect of OMNC on I_{to} was investigated further by analysing its concentration dependence. I_{to} was elicited by a depolarizing pulse to +60 mV from a holding potential of −80 mV. Figure 9A shows superimposed K^+ current traces before and after cumulative superfusion with 3, 10 and 30 μM OMNC. The decay of currents during an activating clamp step in control conditions was well fitted by a single exponential function

$$I_{to}(t) = A_1 \exp(-t/\tau) + A_0 \qquad (5)$$

where A_1 and τ are the initial amplitude and time constant of inactivation, respectively. A_0 is a time-independent component. The average value of the decay time constant (τ) was 48.8±2.7 ms ($n=7$). In the presence of OMNC, the time constant of current decay was decreased. At concentrations higher than 3 μM, a monoexponential relation no longer fitted I_{to} well, on the other hand, a biexponential relation ($I_{to}(t) = A_1\exp(-t/\tau_f) + A_2\exp(-t/\tau_s) + A_0$, where A_1, τ_f, A_2 and τ_s are the initial amplitudes and time constants of fast and slow decaying component of inactivation, respectively) fitted the data well. At 10 and 30 μM, the average value of τ_f was respectively calculated to be 9.1±1.3 ms and 7.3±0.6 ms, which are both significantly shorter than that in control cells ($P<0.001$). The average value of τ_s was respectively calculated to be 42.5±4.4 ms and 51.8±9.5 ms, which are comparable to that in control cells. Since OMNC accelerated the decay time course of I_{to}, the inhibition of I_{to} was evaluated by measuring the integral of the inactivating current ($A_1\exp(-t/\tau)$ or $A_1\exp(-t/\tau_f) + A_2\exp(-t/\tau_s)$) whereas the inhibition of I_{SS} was evaluated by the reduction of the fitted time-independent component (A_0). Figure 9C illustrates the per cent reduction of I_{to} integral and fitted amplitude of I_{SS} as a function of the logarithm of OMNC concentration. The data was fitted with a Hill equation to obtain a concentration-response curve. The mean IC_{50} for I_{to} was 10.4±1.5 μM, with an E_{max} of 100.1±1.9% inhibition and a mean n_H of 1.07±0.10 ($n=10$). The calculated IC_{50} for I_{SS} inhibition by OMNC was 8.7±1.4 μM, with an E_{max} of 101.5±3.0% inhibition and a mean n_H of 1.17±0.17 ($n=8$). The concentration-dependence of inhibition of I_{to} and I_{SS} by quinidine are shown in Figure 9B, D. The calculated IC_{50} for I_{to} inhibition by quinidine was 0.8±0.2 μM (maximal inhibition = 91±2%, $n_H = 1.18\pm0.08$, $n=7$). The calculated IC_{50} for I_{SS} was 0.7±0.1 μM ($E_{max} = 92.9\pm2.2\%$, $n_H = 1.17\pm0.12$, $n=7$).

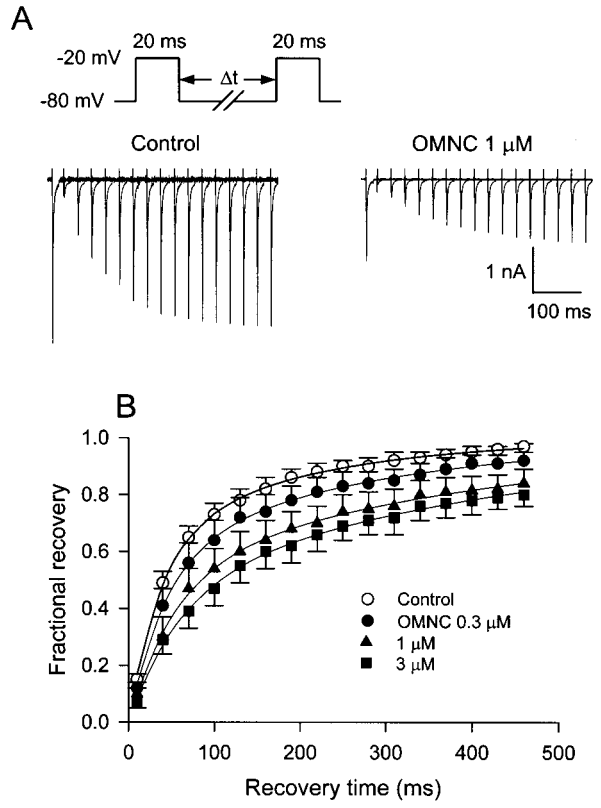

Figure 6 Effects of OMNC on the recovery of I_{Na} from inactivation. (A) The double pulse protocol is shown in the inset. I_{Na} was evoked by a 20 ms test pulse (I_t) to −20 mV at varying intervals after a 20 ms prepulse (I_p) to −20 mV from a holding potential of −80 mV. Records of I_{Na} elicited by the prepulse and the test pulse were superimposed under control conditions (left) and after 5-min superfusion with 1 μM OMNC (right), respectively. (B) Relative values of I_t and I_p (fractional recovery) were plotted along the interpulse interval in the absence and presence of OMNC ($n=8$). The solid lines were best fit of a double exponential function.

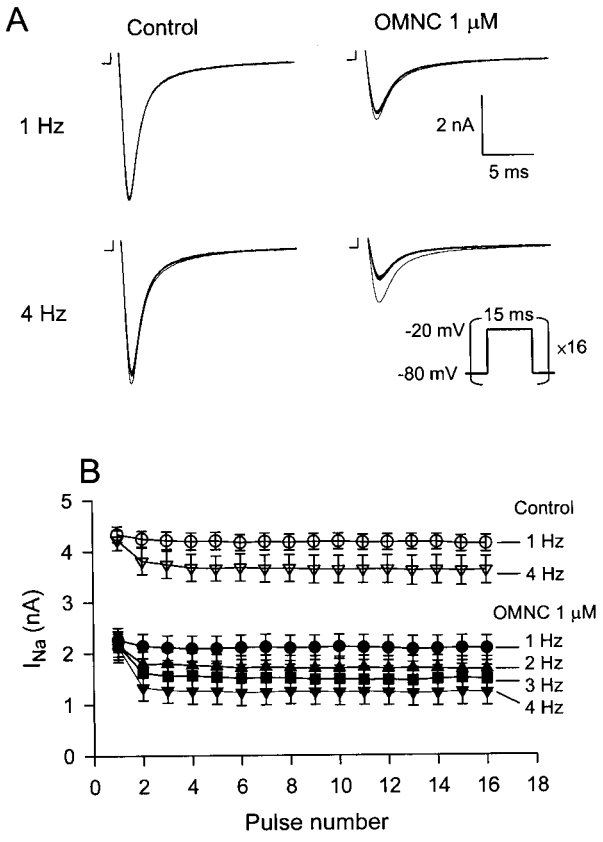

Figure 7 Tonic and use-dependent inhibition of I_{Na} by OMNC. (A) Superimposed records obtained during a train of 16 successive depolarizing pulses applied at a frequency of either 1 or 4 Hz before and during exposure to OMNC (1 μM). The pulse protocol used is shown in the inset of A. (B) Relation between peak I_{Na} and number of pulses applied at different rates under the control and OMNC-application condition. Each data point indicates means±s.e.mean ($n=6$).

Effects of OMNC on steady-state activation, inactivation and recovery from inactivation of I_{to}

Figure 10A shows the voltage dependence of steady-state inactivation and activation curve of I_{to}. The steady-state inactivation was obtained using a conventional double-pulse protocol. Each peak current was normalized to the maximum current measured and plotted as a function of conditioning potential. As shown in Figure 10A, OMNC caused a small hyperpolarization-shift of the steady-state inactivation relationship. On average ($n=7$), $V_h=-28.0\pm4.0$ mV and $k=-4.6\pm0.4$ mV under control conditions, and $V_h=-36.9\pm6.0$ mV and $k=-5.2\pm0.5$ mV ($P>0.05$ for V_h and k) in the presence of 10 μM OMNC and $V_h=-38.0\pm6.0$ mV and $k=-5.3\pm0.4$ mV ($P>0.05$ for V_h and k) in the presence of 30 μM OMNC. The activation curves as shown in Figure 10A were obtained from the normalized conductance of I_{to} channels ($G_{to}/G_{to,\ max}$) which were calculated from the data of I_{to} amplitude in Figure 8A, B. The average values of V_h and k were 1.2 ± 5.7 mV and 12.1 ± 0.7 mV ($n=8$) under control conditions, respectively. OMNC (10 μM) did not affect the voltage dependence for activation ($V_h=-1.5\pm6.8$ mV and $k=13.2\pm1.1$ mV, $P>0.05$ for V_h and k). The effect of OMNC on the recovery kinetics of I_{to} was also examined and is shown in Figure 10B. Recovery from inactivation in the control conditions could be well fitted by a single exponential function. An average value of the recovery time constant was 41.1 ± 1.8 ms ($n=7$). In the presence of 3, 10 and 30 μM OMNC, recovery of I_{to} was significantly prolonged to 49.1 ± 3.4 ms ($P<0.05$), 60.8 ± 6.0 ms ($P<0.01$) and 76.0 ± 5.9 ms ($P<0.001$), respectively.

Modification of the electrophysiological properties of the cardiac conduction system

Changes in the electrophysiological parameters of the cardiac conduction system in 10 rats after cumulative application of OMNC (1–30 μM) are summarized in Table 2. Intracardiac recording detected the atrial activity, His potential, and ventricular activity (Figure 11). The ventricular repolarization time (VRT) was significantly lengthened by OMNC at low concentration (3 μM) and this effect was concentration-dependent. At higher concentrations, the basic cycle length was prolonged (10 μM). The conduction through the AV node (AH interval) and the His-Purkinje system (HV interval) as well as the AV nodal Wenckebach cycle length

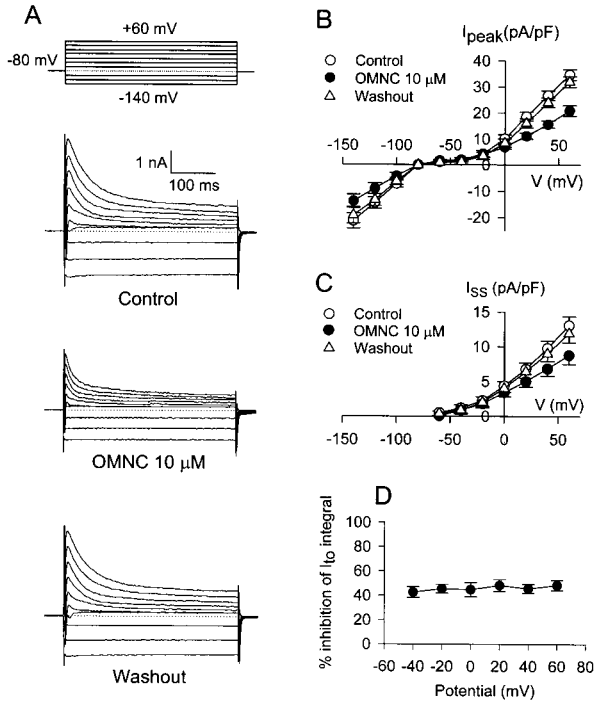

Figure 8 Effects of OMNC on K^+ currents. (A) Families of current traces elicited by a series of 400-ms long depolarizing or hyperpolarizing pulses from a holding potential of -80 mV in the absence and presence of 10 μM OMNC and following washout of the drug. Horizontal dashed line in each panel indicates zero current level. (B) and (C): Averaged $I-V$ relationship for I_{to} (B) and I_{SS} (C) observed in the absence, and presence of 10 μM OMNC, and after washout. (D) Per cent inhibition of I_{to} integral by 10 μM OMNC calculated at different depolarizing potentials. Data points are means$\pm$s.e.mean from eight cells in panel (B), (C) and (D).

were also prolonged (30 μM). The conduction interval through the atrial tissue (SA interval) was not significantly affected. Additionally, OMNC prolonged the atrial and ventricular refractory period at a concentration of 10 μM or higher. At higher concentrations (30 μM), the AV nodal refractory period was also prolonged. In the present experimental protocol the AV node usually became refractory to premature extrastimulation before the His-Purkinje system became refractory. Therefore, only the functional refractory period of the His-Purkinje system (shortest conducted V_1V_2 interval) was measured. It was significantly prolonged at a concentration of 10 μM or higher. As compared to quinidine, OMNC exerted comparable effect on VRT and AERP but less pronounced effects on other parameters (Table 2).

Discussion

In this study, we have demonstrated positive inotropy as well as a significant antiarrhythmic efficacy of a pavine alkaloid derivative, *O*-methyl-neocaryachine (OMNC). The range of effective concentration for conversion of arrhythmias was wide. No new arrhythmias were induced even at a concentration about 10 fold above the EC_{50}. The antiarrhythmic action may be mediated through blockade mainly of the Na^+, I_{to} and I_{SS} channels, and partly through the Ca^{2+} channel. Consequently, OMNC could prolong the conduction intervals and the refractoriness of the cardiac conduction system. The electrophysiological effects were similar to those found for quinidine, a class I_A agent, but were different from it in channel selectivity.

An important consequence of both myocardial ischaemia and reperfusion is the occurrence of various disturbances of cardiac rhythm, including the potential lethal condition of VF (Corr & Witkowski, 1983). The mechanism(s) underlying the genesis of ischaemia reperfusion-induced arrhythmias are complex and controversial. In recent years, a number of factors have been implicated as potential culprits, these include the production of free radicals (Zweier *et al*., 1989) and the consequent electrophysiological disturbances including the reentry and the enhanced automaticity such as oscillatory afterpotentials (Corr & Witkowski, 1983; Manning & Hearse, 1984; Pogwizd & Corr, 1987). Unpublished data has shown that OMNC was found to have no *in vitro* DPPH scavenging activity. This result suggests that the antiarrhythmic action of OMNC may not be due to the free radical scavenging activity.

The results from the present study show that OMNC may exert antiarrhythmic activity by suppression of oscillatory afterpotentials or extrasystole *via* blocking the Na^+ channels. Though the inhibition of action potential upstroke velocity and prolongation of the conduction intervals as well as the refractoriness of the His-Purkinje system and the ventricular tissues may be related with the inhibition of sodium channel (Fozzard, 1990), the effective concentration for slowing the upstroke velocity of papillary muscle is much greater than the IC_{50} for inhibition of I_{Na}. This apparent disparity is due to the inhibition of K^+ outward current which could counterbalance the inhibition of I_{Na}. Another possible explanation for this disparity is that experiments on I_{Na} were studied in low Na^+ (54 mM) solution and lower temperature (25–27°C). However, experiment on V_{max} was performed in normal Tyrode solution and 37°C. Most class I antiarrhythmic agents caused a use-dependent inhibition of I_{Na}, a slower recovery of Na^+ channels from their inactivation state and a negative shift of the voltage-dependent inactivation curve of I_{Na} (Clarkson *et al*., 1988; Grant & Wendt, 1992). In this study, OMNC inhibited I_{Na} with a significant negative shift of the voltage-dependent inactivation curve of I_{Na} but without alteration of the inactivation time constant. In addition, a use-dependent inhibition and a prominent retardation of recovery from inactivation of Na^+ channel were also observed in cells treated with OMNC. According to the modulated receptor hypothesis, the potency of the block of cardiac Na^+ channels by class I agents is different when the channels exist in three different states (resting, activated, and inactivated) (Hondeghem & Katzung, 1977; Hille, 1977). The phenomena of use-dependent block are generally interpreted by drug molecule binding to the open- and inactivated state channels during membrane depolarization. The affinity of OMNC to the inactivated state and resting state Na^+ channels could be estimated by the following equation: $\Delta V_h = k \times \ln[(1+D/K_r)/(1+D/K_i)]$ (Bean *et al*., 1983), where the ΔV_h is the shift in the midpoint, k is the slope factor, D is the drug concentration, and K_r and K_i are the dissociation constants for resting and inactivated Na^+ channels. From the negative shift of V_h obtained in two concentrations of OMNC (1 and 3 μM; Figure 5), the value of K_i and K_r were calculated to be 0.47 μM and 97.7 μM,

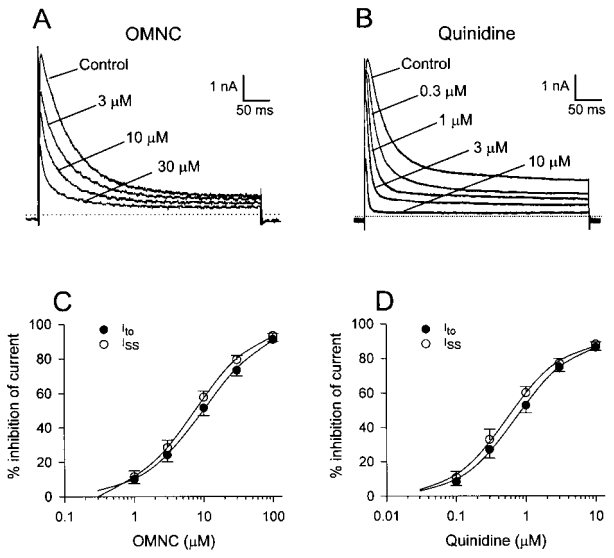

Figure 9 Concentration-dependence of inhibition of K^+ currents by OMNC and quinidine. (A) and (B) Superimposed families of current traces generated by 400-ms depolarizing pulses to +60 mV from a holding potential of −80 mV in the absence or presence of increasing concentrations of OMNC and quinidine, respectively. Horizontal dashed line indicates zero current level. (C) and (D) Concentration-response curve for the effect of OMNC (I_{to}: $n=10$; I_{SS}: $n=8$) and quinidine (I_{to}: $n=7$; I_{SS}: $n=7$) on the integral of I_{to} and the fitted amplitude of I_{SS}. Continuous line was drawn according to the fitting of Hill equation.

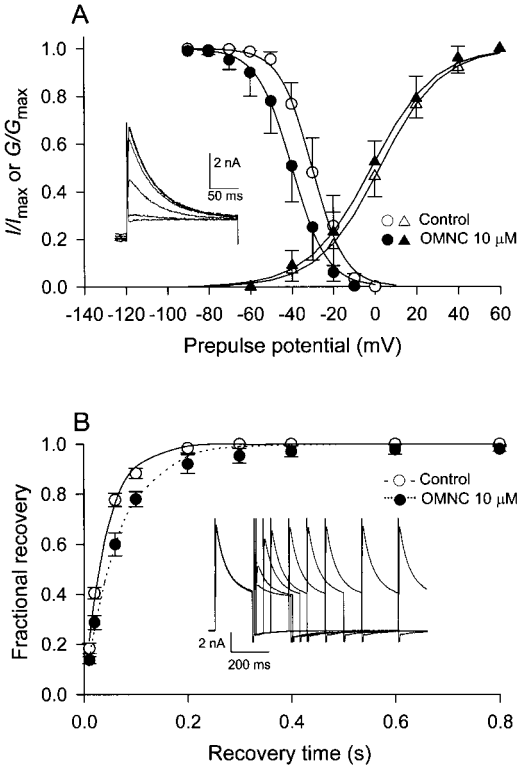

Figure 10 (A) Voltage dependence of steady-state I_{to} activation and inactivation in the absence and presence of 10 μM OMNC. Steady-state inactivation was examined with a double pulse protocol: a conditioning 400 ms pulses to various potentials ranging from −90 to 0 mV was followed by a test depolarizing pulse to +50 mV. The holding potential was −80 mV. The predrug superimposed current traces are shown in the inset. The inactivation curves for I_{to} were obtained by normalizing the current amplitudes (I) to the maximal value (I_{max}) and plotted as a function of the conditioning potentials before and after OMNC ($n=7$). Solid line drawn through the data points were the best fit to the Boltzmann equation. The activation curves were obtained from the normalized conductance of I_{to} channels ($G_{to}/G_{to,\ max}$) which were calculated from the data of I_{to} amplitude in Figure 8A and B and plotted as a function of the depolarizing potentials ($n=8$). Solid line drawn through the data points were the best fit to the Boltzmann equation. (B) Effects of OMNC on reactivation of I_{to}. The twin-pulse protocol used consisted of two identical 200 ms depolarizing pulses to +50 mV from a holding potential of −80 mV. The prepulse-test pulse interval was varied between 10 and 800 ms. An example of recovery of I_{to} from inactivation in control conditions is shown in the inset. The normalized currents (fractional recovery) obtained in the absence and presence of 10 μM OMNC were plotted as a function of the recovery time. Solid and dashed lines represent single exponential fitted to the data in the absence and presence of OMNC ($n=7$), respectively.

respectively. This result suggests that OMNC may bind preferentially to the inactivated channel, which results in a decrease of the available channels for activation. This result may also explain the tonic block of I_{Na} elicited from −80 mV by OMNC. In our previous study, (−)-caryachine, a similar pavine alkaloid as OMNC was found to inhibit I_{Na} with a higher value of K_i (1.2 μM) and lower K_r (48.3 μM) (Chen *et al*., 1996). This result indicates that O-methylation of (−)-caryachine seems to increase the relatively selective binding to inactivated Na^+ channels. The prominent retardation of Na^+ channel recovery from inactivation provides additional evidence that OMNC can interact with inactivated Na^+ channel. Because the time course of inactivation of I_{Na} was unchanged in the presence of OMNC, the rate of transformation of channels from open state to inactivated state may be unaffected by OMNC and the binding of OMNC to channels in open state may be insignificant or not fast enough to affect the time course of I_{Na} inactivation.

In this study, though the potency of OMNC was comparable to quinidine on the inhibition of I_{Na} amplitude, the retardation of I_{Na} recovery and the shifting of inactivation curve, however, were less potent than that of quinidine which had been reported in our previous study (Chang *et al*., 1996). These results together with the multiple mode of action of quinidine on I_{Na} may explain why quinidine was more potent than OMNC on the prolongation of conduction time and refractoriness in the whole heart model. Besides, the action potential V_{max} suppressing effect of quinidine in papillary muscles was stronger than OMNC, this may be explained by the quinidine-induced prominent prolongation of APD which may enhance its inhibitory effect on V_{max}. As judged from the mode of action on I_{Na}, OMNC blocks Na^+ channels in a channel state-dependent manner more like class I_B agents.

Class III and some class I antiarrhythmic agents exert their antiarrhythmic effects by suppressing the K^+ outward currents to prolong the APD and thereby increase the refractoriness of the conduction system and myocardium (Singh & Nademanee, 1985; Hondeghem, 1992). Our result showed that OMNC could suppress the I_{to} and the I_{SS} which consequently prolonged the APD, repolarization time and increased further the refractoriness of the myocardium

Table 2 Concentration-related effects of *O*-methyl-neocaryachine (OMNC) and quinidine on the conduction system of rat isolated perfused hearts

	OMNC (μM)						*Quinidine* (μM)					
	Control	*1*	*3*	*10*	*30*	*Wash*	*Control*	*1*	*3*	*10*	*30*	*Wash*
BCL	276±9	272±9	296±11	304±10*	357±13#	304±15	275±4	284±8	303±10*	357±15#	423±22#	300±10*
SA	10±0	10±0	10±1	11±1	12±1	10±0	8±1	8±1	8±1	9±1	11±1*	8±1
AH	44±3	43±2	44±3	47±4	59±6*	45±4	40±3	43±3	47±4	56±3#	76±4#	41±3
HV	20±1	21±1	21±1	22±1	31±3**	21±1	18±1	19±1	21±1*	26±1#	34±2#	18±0
VRT	69±2	71±2	75±1**	85±3#	105±4#	74±2	60±4	65±5	81±6**	104±6#	122±6#	72±6
WCL	146±6	150±4	153±5	166±10	189±8#	156±5	144±8	152±6	164±5*	189±5#	226±4#	141±6
AERP	37±5	38±3	48±6	71±8**	106±12#	55±10	45±5	44±4	47±7	68±8*	98±8#	64±9
AVNERP	115±4	116±2	119±5	132±11	156±8#	119±5	110±9	114±8	131±7	163±6#	203±4#	108±6
HPFRP	152±4	153±3	164±5	179±11*	215±8#	165±6	149±8	158±5	177±5**	206±4#	243±2#	144±5
VERP	52±3	56±5	63±6	84±7#	125±8#	60±6	32±3	41±3*	56±4#	103±14#	156±13#	41±6

Data (in ms) were obtained from 10 (OMNC group) and nine (quinidine group) experiments and are expressed as means±s.e.mean. Abbreviations: BCL, basic cycle length; SA, sinoatrial conduction interval; AH, atrio-His bundle conduction interval; HV, His-ventricular conduction interval; VRT, ventricular repolarization time interval; WCL, Wenckebach cycle length; AERP: atrial effective refractory period; AVNERP, AV nodal effective refractory period; HPFRP, His-Purkinje system functional refractory period; VERP, ventricular effective refractory period. *$P<0.05$, **$P<0.01$ and #$P<0.001$ as compared with the respective control.

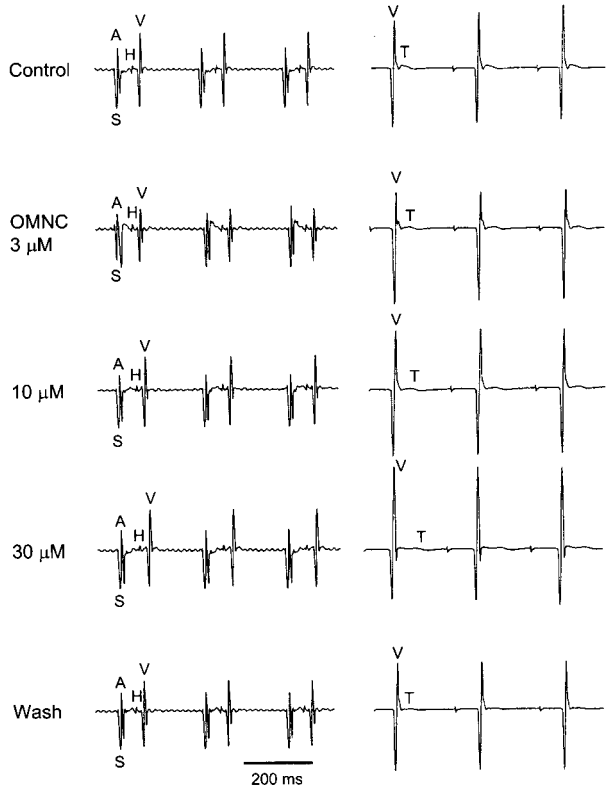

Figure 11 Representative His bundle electrograms (left) and ventricular electrograms (right) after different concentrations of OMNC in the rat heart. The right atrium near the superior vena cava was paced at a constant rate with a pacing cycle length of 250 ms. A: atrial depolarization. H: His bundle depolarization. S: stimulation artifact. T: ventricular repolarization. V: ventricular depolarization. The paper speed was 100 mm/s.

and may therefore contribute to its suppressing effects on the ischaemia/reperfusion-induced tachyarrhythmias. However, the disparity between the effective concentration to prolong the APD of the papillary muscles and to prolong the ventricular repolarization time of isolated hearts was found in this study. This disparity could be explained partly by the heterogeneity in subtypes of I_{to} between papillary muscle and epicardium (Dixon & Mckinnon, 1994; Wickenden *et al*., 1999). Since the heterogeneity in density of I_{to} with a rapid recovery time constant (i.e., Kv 4.2 channels) is a main reason for the regional difference in repolarization time, the stronger inhibition of the component of I_{to} by OMNC may reduce the total dispersion of repolarization in rat heart which may then reduce the incidence of reentrant arrhythmia.

The I_{to} is generally considered an important repolarizing current in the action potential of several mammalian tissues, including human atrium and ventricle (Escande *et al*., 1987; Näbauer *et al*., 1993) and in rat and rabbit cardiac tissues (Josephson *et al*., 1984; Nakayama & Irisawa, 1985; Giles & Imaizumi, 1988). Therefore, I_{to} suppression would increase the refractoriness of atrial, AV nodal and ventricular area. In this study, both OMNC and quinidine block the I_{to} and the I_{SS}, but with different potencies; quinidine is approximately 10-fold more potent than OMNC for the inhibition of both I_{to} and I_{SS}. This result may explain the less marked prolongation of the atrial, atrioventricular and ventricular refractory periods by OMNC than by quinidine. The inhibition of OMNC on I_{to} is characterized by a concentration-dependent increase in the rate of current decay. The acceleration of current decline could be attributed to the binding to open state channels, like quinidine, flecainide and propafenone (Slawsky & Castle, 1994). OMNC tended to shift steady-state inactivation curve of I_{to} to more negative potential suggests that OMNC may partly bind to the inactivated channels which could then result in a decrease of number of resting I_{to} channels available for activation. The retardation of I_{to} recovery in the presence of OMNC may result from the slower dissociation of this agent from their binding sites. As compared to OMNC, previous studies have shown that quinidine also prolonged the recovery of I_{to} from inactivation although the voltage dependent steady-state inactivation curve was not changed (Clark *et al*., 1995; Chang *et al*., 1996).

In diseased human atrial strips, the resting membrane potential of partially depolarized cells is noted to be between −40 and −50 mV, at which I_{to} is partially activated and inactivated, but an incomplete inactivation at this potential

range may result in a residual opening of I_{to} channel which may overlap I_{Ca} (Escande *et al*., 1987). Therefore, it has been proposed that I_{to} plays a protective role in the diseased human atrium by preventing the firing at foci of abnormal automaticity. The present data show that the ratio of IC_{50} for inhibition of I_{to} to IC_{50} for I_{Ca} is 6.4 for quinidine but 0.75 for OMNC. This result indicate that quinidine has relatively selective inhibition of I_{to} which may then result in an increase in generation of abnormal automaticity in partially depolarized myocardium.

Inward rectification of I_{K1} has been suggested to play a major role in the formation of the plateau phase of the cardiac action potential (Lopatin & Nichols, 2001). As the cell repolarizes, the conductance recovers, allowing I_{K1} channels to contribute to repolarization and maintain the resting potential. In rat ventricular myocytes, I_{K1} does not show a negative slope conductance; the decrease of I_{K1} by OMNC may contribute less to an increase in APD. However, the suppression of I_{K1} seems to be responsible for the slight depolarization of the resting potential.

Drugs that block the L-type Ca^{2+} channel may preferentially prolong the conduction and refractoriness of slow response fibres (Harrison, 1985; Fozzard, 1990). Consistent with the modest depressant effect of OMNC on AV nodal conduction time, this agent also prolonged the Wenckebach cycle length (WCL) and AV nodal ERP. This finding suggests that the inhibition of I_{Ca} by OMNC may partially contribute to its antiarrhythmic activity. Drugs that block the Ca^{2+} or Na^+ channels may also result in a negative inotropic effect which is hazardous in some situations (Ravid *et al*., 1989; Schlepper, 1989). Quinidine has been reported to cause a negative inotropic effect and this effect may reside in its significant decrease of I_{Ca} (Nawrath, 1981). In this study, we also observed this phenomenon in rat papillary muscles which were treated with higher concentrations of quinidine although the APD was significantly prolonged at the same time. The positive inotropy of OMNC, another important feature of this compound, was attributed to an inhibition of K^+ channels (an increase in the APD) which is accompanied by a minimal suppression of I_{Ca}. Such modest positive inotropy is important especially in dealing with patients with heart failure.

The potential limitations in this study include that the effects on ionic current were obtained at room temperature and the kinetics of OMNC block and unblock may be substantially different at physiological temperature. Furthermore, since the underlying outward currents (e.g., I_{SS}) which contribute to the repolarization of the rat heart are quite different from that of the human, the electrophysiological effect of OMNC on human heart need be clarified.

In summary, we have identified a satisfactory antiarrhythmic potential for a pavine alkaloid derivative OMNC. This drug has mixed class I and class III properties. However, its channel selectivity, in comparison to quinidine, may give this agent a positive inotropic and less proarrhythmic potential. It was suggested and shown that the combination of Na^+ and K^+ channel-blocking action may be ideal for the development of antiarrhythmic agents selective for ischaemia-dependent arrhythmias (Bain *et al*., 1997). The studies on amiodarone also revealed that classs I_B and class III actions might contribute significantly to the very favourable antiarrhythmic profile of this agent. In fact, combinations of class I and class III features appear to be promising both in terms of antiarrhythmic activity and side effect minimization profiles (Mátyus *et al*., 1997). Therefore, we suggest that OMNC may be a very promising drug for the treatment of cardiac arrhythmias.

This work was supported by research of grants of National Science Council (NSC 88-2314-B-002-123-M48) of Taiwan and CMRP904 from Chang Gung Medical Research Foundation.

References

BAIN, A.I., BARRETT, T.D., BEATCH, G.N., FEDIDA, D., HAYES, E.S., PLOUVIER, B., PUGSLEY, M.K., WALKER, M.J.A., WALKER, M.L., WALL, R.A., YONG, S.L. & ZOLOTOY, A. (1997). Better antiarrhythmics? Development of antiarrhythmic drugs selective for ischemia-dependent arrhythmias. *Drug Dev. Res.,* **24,** 198–210.

BEAN, B.P., COHEN, A.J. & TSIEN, R.W. (1983). Lidocaine block of cardiac sodium channels. *J. Gen. Physiol.,* **81,** 613–642.

CHANG, G.J., WU, M.H., WU, Y.C. & SU, M.J. (1996). Electrophysiological mechanisms for antiarrhythmic efficacy and positive inotropy of liriodenine, a natural aporphine alkaloid from *Fissistigma glaucescens*. *Br. J. Pharmacol.,* **118,** 1571–1583.

CHEN, L., SU, M.J., WU, M.H. & LEE, S.S. (1996). Electrophysiological mechanisms for the antiarrhythmic action of (−)-caryachine in rat heart. *J. Cardiovasc. Pharmacol.,* **27,** 740–748.

CLARK, R.B., SANCHEZ-CHAPULA, J., SALINA-STEFANON, E., DUFF, H.J. & GILES, W.R. (1995). Quinidine-induced open channel block of K^+ current in rat ventricle. *Br. J. Pharmacol.,* **115,** 335–343.

CLARKSON, C.W., FOLLMER, C.H., TEN EICK, R.E., HONDEGHEM, L.M. & YEH, J.Z. (1988). Evidence for two components of sodium channel block by lidocaine in isolated cardiac myocytes. *Circ. Res.,* **63,** 869–978.

CORR, P.B. & WITKOWSKI, F.X. (1983). Potential electrophysiologic mechanisms responsible for dysrhythmias associated with reperfusion of ischemic myocardium. *Circulation,* **68,** 116–124.

CURTIS, M.J. & HEARSE, D.J. (1989). Ischaemia-induced and reperfusion-induced arrhythmias differ in their sensitivity to potassium: implications for mechanisms of initiation and maintenance of ventricular fibrillation. *J. Mol. Cell. Cardiol.,* **21,** 21–40.

DIXON, J.E. & McKINNON, D. (1994). Quantitative analysis of potassium channel mRNA expression in atrial and ventricular muscle of rats. *Circ. Res.,* **75,** 252–260.

ESCANDE, D., COULOMBE, A., FAIVRE, J.-F., DEROUBAIX, E. & CORABOEUF, E. (1987). Two types of transient outward currents in adult human atrial cells. *Am. J. Physiol.,* **252,** H142–H148.

FOZZARD, H.A. (1990). The roles of membrane potential and inward Na^+ and Ca^{2+} currents in determining conduction. In: *Cardiac Electrophysiology: A Textbook*. ed. Rosen, M.R., Janse, M.J., Wit, A.L. pp. 415–425. New York: Futura publishing Co. Inc.

GILES, W.R. & IMAIZUMI, Y. (1988). Comparison of potassium currents in rabbit atrial and ventricular cells. *J. Physiol.,* **405,** 123–145.

GÖZLER, B., LANTZ, M.S. & SHAMMA, M. (1983). The pavine and isopavine alkaloids. *J. Nat. Prod.,* **46,** 293–309.

GRANT, A.O. & WENDT, D.J. (1992). Block and modulation of cardiac Na^+ channels by antiarrhythmic drugs, neurotransmitters and hormones. *Trends Pharmacol. Sci.,* **13,** 352–358.

HAMILL, O.P., MARTY, A., NEHER, E., SAKMANN, B. & SIGWORTH, F.J. (1981). Improved patch-clamp techniques for high resolution current recording from cells and cell-free membrane patches. *Pflügers Arch.,* **391,** 85–100.

HARRISON, D.C. (1985). Antiarrhythmic drug classification: new science and practical applications. *Am. J. Cardiol.,* **56,** 185–187.

HILLE, B. (1977). Local anesthetics: hydrophilic and hydrophobic pathways for the drug-receptor reaction. *J. Gen. Physiol.,* **69,** 497–515.

HONDEGHEM, L.M. (1992). Development of class III antiarrhythmic agents. *J. Cardiovasc. Pharmacol.,* **20**(Suppl. 2): 17–22.

HONDEGHEM, L.M. & KATZUNG, B.G. (1977). Time- and voltage-dependent interactions of antiarrhythmic drugs with cardiac sodium channels. *Biochim. Biophys. Acta,* **472,** 373–398.

JOSEPHSON, I.R., SANCHEZ-CHAPULA, J. & BROWN, A.M. (1984). Early outward current in rat ventricular cells. *Circ. Res.,* **54,** 157–162.

JOSEPHSON, M.E. & SEIDES, S.F. (1979). *Clinical Cardiac Electrophysiology. Technique and Interpretations.* pp. 41–65. Philadelphia: Lea & Febiger.

LOPATIN, A.N. & NICHOLS, C.G. (2001). Inward rectifiers in the heart: an update on I_{K1}. *J. Mol. Cell. Cardiol.,* **33,** 625–638.

MANNING, A.S. & HEARSE, D.J. (1984). Reperfusion-induced arrhythmias: mechanisms and prevention. *J. Mol. Cell. Cardiol.,* **16,** 497–518.

MÁTYUS, P., VARRÓ, A., PAPP, G.J., WAMHOFF, H., VARGA, I. & VIRÁG, L. (1997). Antiarrhythmic agents: current status and prospectives. *Med. Res. Rev.,* **17,** 427–451.

MEISENBERG, G., SIMMONS, W.H. & COLLINS, M.A. (1984). Effects of catecholamine-related mammalian alkaloids on spontaneous and vasopressin-induced behavior in mice. *Pharmacol. Biochem. Behavior,* **20,** 355–360.

MITRA, R. & MORAD, M. (1985). A uniform enzymatic method for the dissociation of myocytes from heart and stomach of vertebrates. *Am. J. Physiol.,* **249,** H1056–H1060.

NÄBAUER, M., BEUCKELMANN, D.J. & ERDMANN, E. (1993). Characteristics of transient outward current in human ventricular myocytes from patients with terminal heart failure. *Circ. Res.,* **73,** 386–394.

NAKAYAMA, T. & IRISAWA, H. (1985). Transient outward current carried by potassium and sodium in quiescent atrioventricular node cells of rabbit. *Circ. Res.,* **57,** 65–73.

NAWRATH, H. (1981). Action potential, membrane currents and force of contraction in mammalian heart muscle fibers treated with quinidine. *J. Pharmacol. Exp. Ther.,* **216,** 176–182.

POGWIZD, S.M. & CORR, P.B. (1987). Electrophysiologic mechanisms underlying arrhythmias due to reperfusion of ischemic myocardium. *Circulation,* **76,** 404–426.

RAVID, S., PODRID, P.J., LAMPERT, S. & LOWN, B. (1989). Congestive heart failure induced by six of the newer antiarrhythmic drugs. *J. Am. Coll. Cardiol.,* **14,** 1326–1330.

SCHLEPPER, M. (1989). Cardiodepressive effects of antiarrhythmic drugs. *Eur. Heart J.,* **10,** E73–E80.

SINGH, B.N. & NADEMANEE, K. (1985). Control of cardiac arrhythmia by selective lengthening of repolarization: Therapeutic considerations and clinical observations. *Am. Heart J.,* **109,** 421–430.

SLAWSKY, M.T. & CASTLE, N.A. (1994). K^+ channel blocking actions of flecainide compared with those of propafenone and quinidine in adult rat ventricular myocytes. *J. Pharmacol. Exp. Ther.,* **269,** 66–74.

THE CARDIAC ARRHYTHMIA SUPPRESSION TRIAL [CAST] INVESTIGATORS. (1989). Preliminary report: effect of encainide and flecainide on mortality in a randomized trial of arrhythmia suppression after myocardial infarction. *N. Engl. J. Med.,* **321,** 406–412.

TOMITA, M., LU, S.T. & IBUKA, T. (1966). Studies on the alkaloids of Formosan lauraceous plants. X. Mass spectrometry of the pavine type alkaloids. *Yagugaku Zasshi,* **86,** 414–417.

WALDO, A.L., CAMM, A.J., DE RUYTER, H., FRIEDMAN, P.L., MACNIEL, D.J., PAULS, J.F., PITT, B., PRATT, C.M., SCHWARTZ, P.J. & VELTRI, E.P. (1996). Effect of d-sotalol on mortality in patients with left ventricular dysfunction after recent and remote myocardial infarction. The SWORD Investigators, Survival With Oral d-Sotalol. *Lancet,* **348,** 7–12.

WELLENS, H.J., BRUGADA, P. & FARRE, J. (1984). Ventricular arrhythmias: Mechanisms and actions of antiarrhythmia drugs. *Am. Heart J.,* **107,** 1053–1057.

WICKENDEN, A.D., JEGLA, T.J., KAPRIELIAN, R. & BACKX, P.H. (1999). Regional contributions of Kv1.4, Kv4.2, and Kv4.3 to transient outward K^+ current in rat ventricle. *Am. J. Physiol.,* **276,** H1599–H1607.

WOOSLEY, R.L. (1991). Antiarrhythmic drugs. *Annu. Rev. Pharmacol. Toxicol.,* **31,** 427–455.

WU, Y.C., LIOU, Y.F., LU, S.T., CHEN, C.H., CHANG, J.J. & LEE, K.H. (1989). Cytotoxicity of isoquinoline alkaloids and their *N*-oxides. *Planta Med.,* **55,** 163–165.

ZWEIER, J.L., KUPPUSAMY, P., WILLIAMS, R., RAYBURN, B.K., SMITH, D., WEISFELDT, M.L. & FLAHERTY, J.T. (1989). Measurement and characterization of postischemic free radical generation in the isolated perfused heart. *J. Biol. Chem.,* **264,** 18890–18895.

(Received January 15, 2002
Revised March 19, 2002
Accepted March 25, 2002)